

ARTICLE

Assessment of Mangrove Cover Change Based on Combining Remote Sensing Technique and Hydrodynamic Model Simulation

Nguyen Van Thinh ^{1*} , Ngo Trung Dung ¹, Nguyen Trong Hiep ¹, Do Phong Luu ¹, Dang Truong An ^{2,3}

¹ Joint Vietnam - Russia Tropical Science and Technology Research Center, Ho Chi Minh City 700000, Vietnam

² Department of Oceanology, Meteorology and Hydrology, University of Science, Ho Chi Minh City 700000, Vietnam

³ Viet Nam National University-Ho Chi Minh, Ho Chi Minh City 700000, Vietnam

ABSTRACT

Mangrove ecosystems along Vietnam's coastline face significant degradation due to human activities, despite their crucial role in coastal protection against natural hazards. This study aims to assess the spatial and temporal changes in mangrove coverage along Vietnam's southern coast by integrating remote sensing techniques with hydrodynamic model simulations. The research methodology combines the Collect Earth tool analysis of Spot-4 and Planet satellite imagery (2000–2020) with Mike 21-HD two-dimensional (2D) hydrodynamic modeling to evaluate mangrove coverage changes by simulating shoreline erosion. Results analysis reveals that a significant increase of 109.83 ha in mangrove area within Vinh Chau Town of Soc Trang Province during the period 2010–2020, predominantly in the eastern region. Hydrodynamic simulations demonstrate that the coastal zone is primarily influenced by the interaction of nearshore currents, East Sea tides, and seasonal monsoon wave patterns. The model results effectively capture the complex interactions between these hydrodynamic factors and mangrove distribution. These findings not only validate the effectiveness of combining remote sensing and hydrodynamic modeling for mangrove assessment but also provide crucial insights for sustainable coastal ecosystem management. The study's integrated approach offers a robust framework for monitoring mangrove dynamics and developing evidence-based conservation strategies, highlighting the importance of maintaining these vital ecosystems for coastal protection.

Keywords: Mangrove; Wave; Current; Hydrodynamic Modeling; Satellite

*CORRESPONDING AUTHOR:

Nguyen Van Thinh, Joint Vietnam - Russia Tropical Science and Technology Research Center, Ho Chi Minh City 700000, Vietnam;
Email: thinh39b@gmail.com

ARTICLE INFO

Received: 8 November 2024 | Revised: 19 November 2024 | Accepted: 25 November 2024 | Published Online: 24 January 2025
DOI: <https://doi.org/10.30564/jees.v7i2.7730>

CITATION

Van Thinh, N., Dung, N.T., Hiep, N.T., et al., 2025. Assessment of Mangrove Cover Change Based on Combining Remote Sensing Technique and Hydrodynamic Model Simulation. *Journal of Environmental & Earth Sciences*. 7(2): 151–160. DOI: <https://doi.org/10.30564/jees.v7i2.7730>

COPYRIGHT

Copyright © 2025 by the author(s). Published by Bilingual Publishing Group. This is an open access article under the Creative Commons Attribution-NonCommercial 4.0 International (CC BY-NC 4.0) License (<https://creativecommons.org/licenses/by-nc/4.0/>).

1. Introduction

Mangroves are among the most productive ecosystems on Earth, providing diverse ecological, biophysical, and socio-economic functions^[1]. These coastal forests play a crucial role in protecting coastlines against natural hazards such as storms, typhoons, tsunamis, and coastal erosion through their remarkable ability to reduce wave energy^[2, 3]. This protective function is achieved through their complex root networks, which hold sediments and slow down the formation of tidal waves^[4, 5]. Beyond coastal protection, mangroves deliver various ecosystem Services^[4, 5], including both direct economic values such as timber and fisheries and indirect environmental benefits such as carbon sequestration and water quality improvement^[6, 7]. However, these vital ecosystems face severe threats globally from human activities, including logging, urbanization, tourism development, plastic pollution, heavy metals, and oil spills^[8, 9]. The degradation of mangrove ecosystems diminishes their capacity to provide essential services such as flood control, drought mitigation, biodiversity conservation, and natural resource provision^[10, 11]. Even in the world's largest wetland, Pantanal, mangroves are experiencing severe impacts from drought and wildfires, pushing some species toward extinction^[7, 12].

In Vietnam, the situation is particularly concerning, with mangrove coverage showing a dramatic decline over the past decades^[9, 13]. The area has decreased from 408,500 ha in 1943 to 155,290 ha in 2000, representing an approximately 80% reduction over 60 years^[10, 14]. Among the factors causing the decline of mangrove area, coastal erosion due to hydrodynamic factors have been identified as key factors in this decline^[14, 15], with erosion rates ranging from 4 meters per year in river mouths to 50 meters per year in coastal areas^[8, 9, 15]. Hong et al.^[10] reported that mangroves significantly reduce wave height, showing a 75–85% reduction from 1.3 m to 0.2 m when waves enter mangrove areas. A study by Mazda et al.^[14] demonstrated enhanced wave energy reduction at high water depths due to the spreading of branches and leaves.

Modern monitoring approaches using remote sensing and GIS technologies have revolutionized the study of mangroves covering changes and wetland areas globally^[12, 15–17]. With over 300 satellites from more than 15 countries currently observing Earth^[18, 19], these methods offer advan-

tages over traditional monitoring approaches, which are often time-consuming, labor-intensive, and limited in spatial coverage^[19]. High-resolution satellite imagery has been particularly valuable in mangrove cover change studies, as demonstrated by numerous studies utilizing various satellite platforms^[20–25]. Song et al.^[19] demonstrated the effectiveness of Spot 6 imagery in analyzing chlorophyll-a concentrations at Kristalbad, a man-made wetland in the Netherlands. Various satellite platforms, including Formosat-2, Spot 6, Sentinel-2MSI, and Landsat-8, have been successfully integrated with traditional hydrological models for water area monitoring^[21–27]. The temporal analysis of mangrove areas through satellite imagery enables comprehensive assessment of both natural and anthropogenic impacts on these ecosystems, thereby informing effective conservation and development strategies. This study aims to assess spatial and temporal changes in mangrove coverage in the coastal mangrove of Vinh Chau Town belonging to the southern coast of Vietnam. The assessment will be based on satellite image analysis combined with hydrodynamic model simulation. This study is expected to provide valuable information on the current status of mangrove coverage in the study area and will contribute to the development of effective conservation and management strategies for mangrove ecosystems in Vietnam.

2. Materials and Methods

2.1. Study Area

The Mekong Delta coastal region is located in southwestern Vietnam (7°57'–11°10' N latitude and 105°15'–106°53' E longitude), along the Gulf of Thailand and East Sea (**Figure 1**). The coastal region's topography is characterized by a flat and low-lying terrain, with an average elevation of less than 2 meters above mean sea level^[28]. The coastal area of the Mekong Delta is mainly influenced by the two northeast and southwest monsoon seasons^[27]. The northeast monsoon typically prevails from November to March, dominating significant water level fluctuations due to tides, with varying tidal ranges between the eastern and western sides of the Mekong Delta^[28]. During this period, the wind and wave directions are predominantly from the northeast or east^[11, 28]. In contrast, the southwest monsoon sets in from May to September, characterized by winds and

waves primarily originating from the southwest^[28, 29]. As a result, the seasonal wave regimes and coastal currents, which are influenced by waves, undergo notable changes between the northeast and southwest monsoon Seasons^[11, 28].

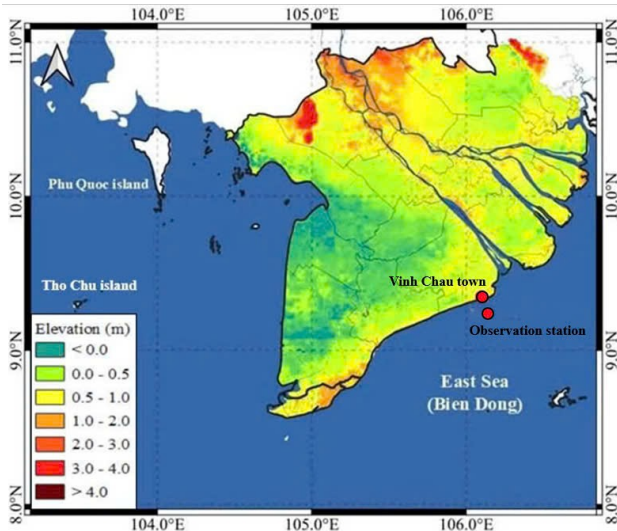


Figure 1. Map of the coastal region of Mekong Delta with study position marked in red circle.

During the wet season, the region experiences strong winds and high waves, whereas the dry season is characterized by light winds and calm seas^[28]. The region’s unique geography features make different tidal ranges between eastern and western sides, contributes to the dynamic environment for both ecological and economic development, with a rich biodiversity and significant mangrove coverage^[8, 11, 15].

2.2. Data Collection

2.2.1. Hydrodynamic Data Collection

Shoreline and bathymetric data were collected to establish the computational domain while hydrodynamic parameters were measured to simulate hydrodynamic processes (Figure 2). The shoreline data were extracted using Google Earth imagery from 2023 and digitized using ArcGIS software. The bathymetric setup supporting the MIKE 11 (1D) hydrodynamic model simulation was measured using an Echo-Sounder. Wave height, current speed and direction data were measured using a wave and current gauge (Nortek Signature ADCP 1000) while water level was monitored

using a self-recording water level measuring device (Solinst 3001 LTC Leve logger). Cross-sections and river network data were obtained from the annually updated database of the Southern Institute of Water Resources Research (SI-WRR). The bathymetric data was converted to UTM Zone 48 coordinate system to ensure synchronization with GIS data. For the bathymetric map configuration supporting the MIKE 21-HD (2D) hydrodynamic model simulation, relevant data were collected through field surveys conducted from 00:00 on June 18, 2023, to 12:00 on June 30, 2023, in the coastal region of Vinh Chau Town, Soc Trang Province, and from 00:00 on May 1, 2023, to 12:00 on June 29, 2023. The simulated results for the entire southern coast river network using the MIKE 11 model were extracted the flow discharge and water level at required locations to establish boundary conditions for the MIKE 21-2D hydrodynamic model simulation.

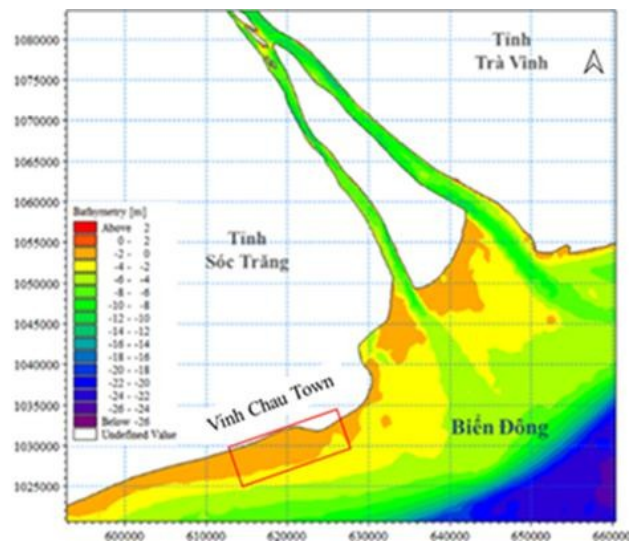


Figure 2. Bathymetric map of the coastal zone of Vinh Chau Town, Soc Trang Province

2.2.2. Satellite Image Data Collection

In this study, we utilized Spot-4 satellite imagery from 2000 and 2010, and Planet satellite imagery from 2020 to create land cover maps for two distinct mangrove areas, including the coastal mangrove in Vinh Chau Town, Soc Trang Province, representing coastal mangrove ecosystems (Table 1).

Table 1. Satellite image parameters including image types, spectral channel and spatial resolution during the period 2000–2020.

Image Types	Spectral Channel	Spatial Resolution
Spot-4	Pan (610–680 nm)	Panchromatic: 10 m × 10 m Multispectral: 20 m × 20 m
	Green (500–590 nm)	
	Red (610–680 nm)	
	Near IR (780–890 nm)	
	SWIR (1,530–1,750 nm)	
Spot-4	Blue (0.455–0.525 μm)	Panchromatic: 10 m × 10 m Multispectral: 20 m × 20 m
	Green (0.530–0.590 μm)	
	Red (0.625–0.695 μm)	
	Near-Infrared (0.760–0.890 μm)	
	Blue (0.455–0.525 μm)	
Planet	Green (0.530–0.590 μm)	4.7 m × 4.7 m
	Red (0.625–0.695 μm)	
	Near-Infrared (0.760–0.890 μm)	

2.3. Approach Methods

2.3.1. Processing Satellite Images

Satellite image processing and analysis were conducted applying the multiresolution algorithm to perform image segmentation and interpretation based on eCognition (Version 9.1) software^[29, 30]. This process facilitated the creation of wetland land cover maps for the study area using multi-temporal satellite imagery, including SPOT- 4 (2000, 2010) and Planet (2020).

Specifically, the image interpretation key samples (IKS) for 2020 were processed through Collect Earth tool, with 80% of the samples allocated for post-segmentation state assignment and the remaining 20% reserved for field verification and accuracy assessment^[30, 31]. For the 2000 and 2010 IKS, historical Google Earth imagery served as the primary reference for interpretation through Collect Earth tool. The image segmentation process utilized the multiresolution segmentation algorithm, originally developed by Baatz^[31]. This algorithm employs a bottom-up region-merging technique that groups similar pixels and their neighbors into objects based on homogeneity criteria^[30, 31]. As demonstrated by Kavzoglu^[29], the segmentation process creates objects by grouping spectrally similar characteristics in the imagery. The spectral or color heterogeneity is defined by the formula^[29]:

$$T_s = \max T_m, \text{ with } 1 \leq m \leq n \quad (1)$$

To define the discontinuity data points, which relate to the value points when T_s reaches the maximum value in the observation data series. Where, T_m in Equation (1) is

defined by Equation (2)^[29]:

$$T_m = \bar{m} z_1 + (n - m) \bar{z}_1, \quad (2)$$

with $m = 1, 2, 3, \dots, n$

And z_1 in the Equation (2) is defined by Equation (3).

2.3.2. Processing Hydrodynamic Parameters

In this study, flow discharge and water level at the cross-sections were obtained from 1D hydraulic model simulations, which were used as boundary and initial conditions for the MIKE 21 hydrodynamic model (2D). Additionally, hydrodynamic parameters in the Mekong Delta coastal zones were measured to be used for simulating the MIKE 21 hydrodynamic model (2D). Wave, current speed, water level and wind data were collected during the northeast monsoon season and southwest monsoon season at the coast zone of the study area.

3. Results and Discussion

3.1. Model Performance Assessment

The model performance assessment was based on the agreement of the overall shape of the time series of water level and current speed with the value of the statistical indices such as the Nash–Sutcliffe (NASH) criterion which described by Nash and Sutcliffe (1970), Root Mean Square Error (RMSE) applied by Fleming^[30] and the goodness of fit (R^2)^[30]. According to, NASH and RMSE are the two criteria widely used to assess the simulated results from hydrodynamic model with observed data^[30]. The NASH index has been used to detect systematic errors for long term simulation. The NASH index was developed to evaluate the

percentage of accuracy of simulated results compared with observed data. NASH index is described as follows^[30]:

$$NASH = \frac{\sum_{i=1}^n (q_0 - q_m)^2 - \sum_{i=1}^n (q_0 - q_s)^2}{\sum_{i=1}^n (q_0 - q_m)^2} \quad (3)$$

where q_0 is the observed data, n is the number of data points, q_m is the mean value of the observed data, q_s is the simulated result, while the RMSE can be regarded as a measure of absolute error between the simulated model and observed data. RMSE is described as follows^[30]:

$$RMSE = \sqrt{\frac{1}{n} \sum_{i=1}^n (q_0 - q_s)^2} \quad (4)$$

where q_0 is the observed data, q_s is the simulated result, n is the number of data points

The model performance for hydrodynamic simulation showed satisfactory result if the values of NASH index and R^2 greater than 0.5. While the RMSE indicated a perfect match between observed data and simulated model if the values of RMSE equals zero and can be considered satisfactory if the value of RMSE is less than 0.5.

To evaluate the performance of the Mike 21HD hydrodynamic model, we compared the simulated results from the applied model with observed data at the coastal area of Vinh Chau Town, Soc Trang Province in the northeast and southwest monsoon season. The comparison of water level simulations with observed data revealed a high degree of reliability, with a NASH of 0.95, an RMSE of 0.19, and R^2 of 0.98. These statistics indicate a strong agreement between simulated and observed water levels (**Figure 3** and **Table 2**).

Similarly, the comparison of current speed simulations with observed data showed a moderate level of agreement, with a NASH index of 0.46, an RMSE of 0.04, and an R^2 of 0.63. Overall, the model performance demonstrated an agreement between simulated and observed water levels and current speeds (**Figure 3** and **Table 2**).

The results of this analysis show that the performance of the hydrodynamic model has been evaluated highly, particularly in simulating water levels. The model has demonstrated a high degree of agreement with observed data, indicating the reliability of the model in simulating hydrodynamic characteristics. However, the performance of the model in simulating current speed was not as high as water levels but still showed a moderate level of agreement.

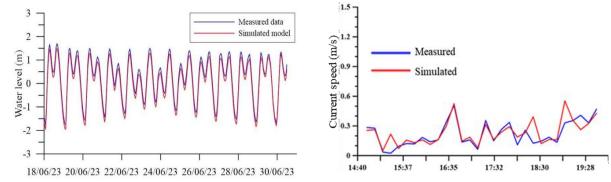


Figure 3. Comparison of the simulated model water level with the measured data of the coastal station during the project’s surveys and comparison of the simulated model coastal current speed with the ADCP data of the coastal observation station. The observation data contains current speed and direction. **Figure 3** shows a generally good match between the simulated model and measured data with NASH = 0.46, RMSE = 0.04 and $R^2 = 0.63$ for current speed, and NASH = 0.95, RMSE = 0.19 and $R^2 = 0.98$, respectively for water level.

Table 2. Model performance for simulating water level and current speed at the coastal region of Vinh Chau Town, Soc Trang Province.

Index	Water Level	Current Speed
NASH	0.95	0.46
RMSE	0.19	0.04
R^2	0.98	0.63

3.2. Simulation Results of Hydrodynamic Characteristics in the Northeast Monsoon

The simulation results for the hydrodynamic characteristics (waves, current speed, and water level fluctuations) of the coastal area of Vinh Chau Town, Soc Trang province during the northeast monsoon is compared with field measurements, as shown in **Figures 4** and **5**.

Due to the location of the study area adjacent to the East Sea and the seafloor topography, the waves in this area mainly propagate in a direction parallel to the coastline towards the east and southeast. With relatively stable wind speed and strong current speed dispersion, the wave field in the study area is not large (**Figure 4**).

The simulation results from the Mike 21HD model show that the water level fluctuations at the coast area of Vinh Chau Town, Soc Trang province are mainly dominated by the East Sea tidal regime with a semi-diurnal tide. The measured water level fluctuated within the range of 3.6–4.1 m, with an average measured water level of approximately 3.8 m. This indicates that the water level fluctuation is irregular and relatively high during the northeast monsoon. While the simulated results for the current speed field are also small and consistent with the actual survey results of the study area. The simulated current speed field shows that the study area has a current distribution range of 0.1–0.4

m/s, with an average current speed of approximately 0.2 m/s, and the simulated results from the hydrodynamic model are consistent with the actual measured data with a correlation coefficient of approximately 0.62. The simulated results of wave height were relatively small, with the significant wave height varies mainly within the range of 0.2 m to 0.4 m, with a frequency of occurrence of 45% while the maximum significant wave height recorded at 0.6 m (Figure 4). In the Southwest monsoon wind direction towards the shore. In general, the simulation results for the hydrodynamic characteristics in the coastal area of the study area is consistent with the actual survey results in the Northeast monsoon.

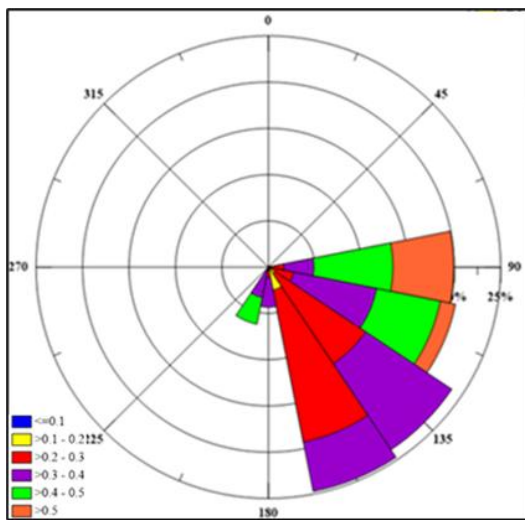


Figure 4. Simulation results of wave height distribution at the coastal area of Vinh Chau Town, Soc Trang Province during the northeast monsoon.

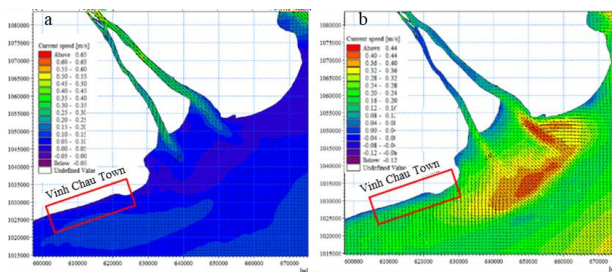


Figure 5. Simulation results of current speed distribution during a) the high tide phase, b) low tide phase at Vinh Chau Town in the northeast monsoon

3.3. Simulation Results of Hydrodynamic Characteristics in the Southern Monsoon

The simulation results for the hydrodynamic characteristics of the coastal area of Vinh Chau town, during the

Southwest monsoon, are presented in Figures 6 and 7. The analysis shows that the significant wave height varies mainly within the range of 0.4 m to 0.6 m, with a frequency of occurrence of nearly 80%, with the maximum significant wave height recorded at 0.8 m (Figure 6). In combination with the wind pattern, it is clear that the wave direction is mainly parallel and oblique to the coastline in the direction of Southwest. The simulated results show that the wave direction changes due to the influence of the seafloor topography, resulting in an oblique direction to the shore. The simulated results of water level fluctuation are range between -1.75 m and 1.70 m, with a semi-diurnal tide that is affected by the tidal regime characteristic of the East Sea. The simulated current speed field shows that the study area has a current distribution range of $0.1-0.4$ m/s, with an average current speed of approximately 0.2 m/s, and the simulated results from the models are consistent with the actual measured data.

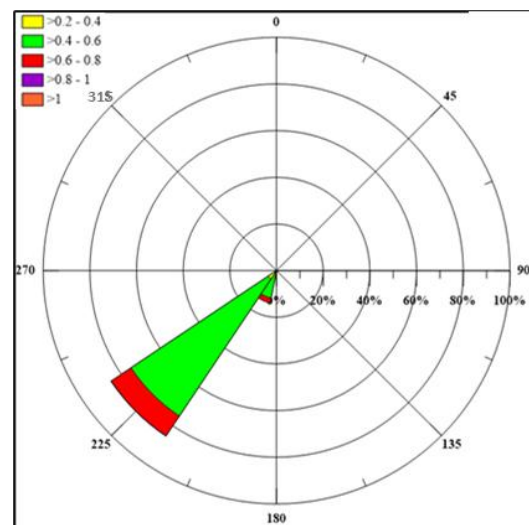


Figure 6. Simulation results of wave height distribution at the coastal region of Vinh Chau Town, Soc Trang Province in the southwest monsoon.

Due to the location of the study area adjacent to the East Sea and the seafloor topography, the waves in this area mainly propagate in a direction parallel to the coastline towards the east and southeast. With relatively stable wind speed and strong current dispersion, the wave field in the study area is not large (Figure 6). In general, the simulation results from the Mike 21HD model show that the water level fluctuations the coast area of Vinh Chau Town are mainly dominated by the East Sea tidal regime with a semi-diurnal tide, while the simulated results for the current speed field and significant wave height are also small and consistent

with the actual survey results of the study area. In general, the coastal dynamics at the study area are mainly dependent on the coastal current speed, East Sea tidal regime, and wave pattern, which are influenced by the two monsoon seasons, Northeast and Southwest.

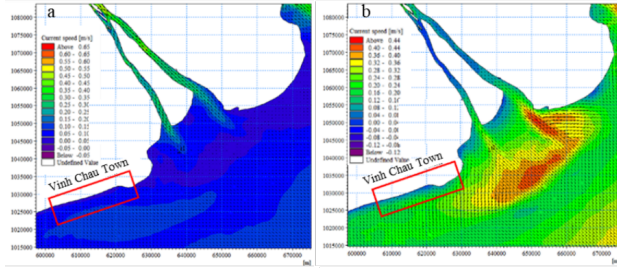


Figure 7. Simulation results of current distribution during a) the high tide phase, b) low tide phase at Vinh Chau Town in the southwest monsoon.

3.4. Changes in Mangrove Cover in the Study Areas during the Period 2000–2020

In Vinh Tan commune, Vinh Chau district, mangroves are concentrated in the south of the study area. The total area of mangrove in Vinh Tan commune is 142.1 ha, with the dominant species being *Avicennia alba*, *Rhizophora stylosa*, *Sonneretia alba*, *Avicennia marina*, *Avicennia officinalis*, *Heritiera littoralis* and *Lumnitzera racemosa* (Table 3, Figure 8). In other neighboring areas, the main types of land cover are agricultural land, residential land, water bodies, and aquaculture area, with a total area of 5,204.9 ha (Table 3). This reveals the important role of mangroves in this area, as they are considered as breakwaters and minimize the effects of wave height, storm surge and other natural disasters.

Table 3. Temporal variation of vegetation covers across the study area in the period 2000–2020.

Cover Types	2000		2010		2020		Changed Cover		Trends
	Area (ha)	(%)	Area (ha)	(%)	Area (ha)	(%)	2000–2010 (%)	2010–2020 (%)	2000–2020 (%)
Mangrove	112.9	2.1	32.3	0.6	142.1	2.6	-1.5	2.0	0.5
Other land	3680.7	68.8	3695.0	69.1	3695.0	69.1	0.2	0.0	0.2
Water body	1553.3	29.0	1619.9	30.2	1509.8	28.2	1.2	-2.0	-0.8
Total	5346.9	99.9	5347.2	99.9	5204.8	99.9	-	-	-

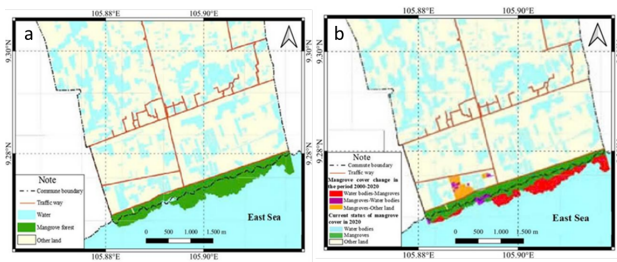


Figure 8. Map of a) mangrove cover in current status of 2020 and b) mangrove cover change in the period 2000–2020 in the coast region of Vinh Chau Town, Soc Trang province.

During the period 2000–2020, the mangrove area increased by 29.1 ha in 20 years, equivalent to an increase of about 25.8%, showing effective efforts to protect and maintain mangroves, effective environmental protection and mangrove restoration policies. Mangroves play an important role in protecting the coast and preventing erosion. Other land areas only increased slightly by 14.3 ha, equivalent to 0.3%. This change may come from the conversion of other land types to diverse uses but is not large enough to create a significant change in the total area (Table 3). The period from 2010–2020 witnessed a significant increase in

mangrove areas. In 10 years, the area of mangrove forest increased from 32.3 ha to 142.1 ha. This reflects that the policies and programs for restoring mangrove ecosystems have achieved high efficiency. The mangrove grows well and is less affected by hydrodynamic factors, extending to the sea in the south of the study area (Figure 8, Table 3).

Overall, the integration of hydrodynamic modeling and remote sensing analysis revealed significant correlations between mangrove coverage changes and coastal hydrodynamic processes. The observed increase of 109.83 ha in mangrove area during 2010–2020 predominantly occurred in regions where the hydrodynamic model showed moderate wave heights (0.2–0.4 m) and stable current speeds (0.1–0.4 m/s). This correlation suggests that these hydrodynamic conditions create favorable environments for mangrove establishment and growth. The model’s simulation of seasonal variations in wave patterns and current distributions provides crucial insights into why mangrove expansion was more successful in the eastern region. Furthermore, the combined approach demonstrated that areas with semi-diurnal tidal pat-

terns and stable current dispersion exhibited better mangrove survival rates. These findings validate the effectiveness of integrating remote sensing and hydrodynamic modeling for understanding mangrove ecosystem dynamics, providing a robust framework for future coastal management strategies.

4. Conclusions

Analysis of satellite imagery data reveals changes in mangrove forest coverage in Vinh Chau Town, Soc Trang Province, with a notable increase of 109.8 hectares during the 2010–2020 period, primarily concentrated in the eastern part of the study area.

The results of the calibration of the wave height and the water level show a good consistency in phase and magnitude, indicating that the Mike-21HD 2D hydrodynamic modeling is consistent with the actual conditions across the coast region of the study area. In the coastal area of Vinh Chau Town, the variation of the coastline is mainly dependent on the tidal currents, the East Sea tide regime, and the wave regime, which are influenced by the two monsoon seasons, the Northeast and Southwesterly monsoons. There is a phenomenon of water flooding along the coast during the rising tide periods due to the combination of the tidal currents and waves.

Hydrodynamic regime simulations using the MIKE 21HD model demonstrate that the coastal zone of Vinh Chau Town is predominantly influenced by coastal currents, East Sea tides, and wave patterns during the Northeast and Southwest monsoon seasons. The relatively low values of waves, currents, and tides have minimal impact on the coastline in these study areas. This stability is primarily attributed to due to the geographical location and the morphological characteristics of the coastal area's beach which is quite gentle. The hydrodynamic simulation results align well with the actual coastal morphology of the study area. The study of mangrove forest area dynamics, through the integration of remote sensing techniques and hydrodynamic model simulation, enables the proposal of solutions for maintaining and sustainably developing this coastal ecosystem.

The findings of this study have significant implications for the conservation and management of mangrove ecosystems along the southern coast of Vietnam. The study's results demonstrate the importance of protecting and restoring mangroves to maintain their ecological and economic benefits.

Additionally, the study's findings highlight the need for sustainable management and development of mangrove ecosystems, which can be achieved through the implementation of effective conservation and restoration strategies.

Author Contributions

Conceptualization: N.V.T. and N.T.D.; Data curation: N.V.T., N.T.H., D.P.L., N.T.D., M.Q.T.; writing—original draft preparation: N.T.D., N.V.T. and D.T.A.; writing—review and editing: N.V.T. and D.T.A. All authors have read and agreed to the published version of the manuscript.

Funding

This research was supported by Environmental Protection Project 2023–2024, with the Joint Vietnam - Russia Tropical Science and Technology Research Center (Southern Branch) as the lead Institution. The authors would like to express their sincere gratitude to PhD. Nguyen Cong Thanh for his support in the hydrodynamics survey content.

Institutional Review Board Statement

Not applicable.

Informed Consent Statement

Not applicable.

Data Availability Statement

The data supporting the findings of this study have been generated but are not currently available in a public repository. The data can be made available by the corresponding author upon reasonable request.

Acknowledgments

This research was supported by Defense's Environmental Protection Project 2023–2024, with the Southern Branch/Joint Vietnam - Russia Tropical Science and Technology Research Center as the lead institution. The authors would like to express their sincere gratitude to PhD. Nguyen Cong Thanh for his support in the hydrodynamics survey

content.

Conflicts of Interest

The authors declare that this manuscript represents original work that has not been published previously and is not under consideration for publication elsewhere. The research was conducted by the author team without any plagiarism from previous studies. There are no conflicts of interest among the authors.

References

- [1] Bherwani, H., Niwalkar, A., Kapley, A., Biniwale, R., 2024. Mapping and valuation of ecosystem services of mangroves: a detailed study from the Andaman Island. *Landscape and Ecological Engineering*. 21, 1–12.
- [2] FAO, 2007. *The World's Mangroves 1980-2005*. FAO Forestry Paper 153. 30 December 2007.
- [3] Cunningham, E., 2019. *The role of mangroves in coastal protection*. Wood Environment & Infrastructure Solutions UK Limited. Doc Ref: 41607rep03i1
- [4] Mukherjee, N., Sutherland, W., Dicks, L., Hugé, J., Koedam, N., Dahdouh-Guebas, F., 2014. Ecosystem Service Valuations of Mangrove Ecosystems to Inform Decision Making and Future Valuation Exercises. *PloS one*. 9(9). e107706.
- [5] Zeng, H., Jia, M., Zhang, R., Wang, Z., Mao, D., Ren, C., Zhao, C., 2023. Monitoring the light pollution changes of China's mangrove forests from 1992-2020 using nighttime light data. *Frontiers in Marine Science*. 10, P.1187702. DOI: <https://doi.org/10.3389/fmars.2023.1187702>
- [6] Riddin, T., Adams, J., Rajkaran, A., Machite, A., Peer, N., Suarez, E., 2024. IUCN Red List of Ecosystems, Mangroves of The Agulhas. Available from: <https://doi.org/10.32942/X2H322> (Cited 01 June 2024)
- [7] Berlinck, C., Lima, L.H.A., Pereira, A.M.M., Carvalho Jr, E.A.R., Paula, R.C., Thomas, W.M., Morato, R.G., 2021. The Pantanal is on fire and only a sustainable agenda can save the largest wetland in the world. *Brazilian Journal of Biology*. 82(42), e244200.
- [8] Phan, L.K., van Thiel de Vries, J.S., Stive, M.J., 2015. Coastal Mangrove Squeeze in the Mekong Delta. *Journal of Coastal Research*. 31(2), 233–243.
- [9] Linh, P.K., Son, T.H., 2021. Hydrodynamic characteristics and the role of mangrove forests in coastal erosion protection and climate change adaptation in the Mekong Delta. *Journal of Water Resources Science and Technology*. 66, 1–11.
- [10] Hong, P.N., 1999. *Vietnam's Mangrove Forests*. Agriculture Publishing House: Hanoi, p. 173.
- [11] Mazda, Y., Magi, M., Kogo, M., Hong, P.N., 1997. Mangroves as a coastal protection from waves in the Tong King delta, Vietnam. *Mangroves and Salt Marshes*. 1(2). 127–135.
- [12] O'Leary, F., 2022. Wetland loss in the Ñeembucú Wetlands Complex, Paraguay, using remote sensing. DOI: <https://doi.org/10.1101/2022.01.03.474818>. Available from: <https://www.biorxiv.org/content/10.1101/2022.01.03.474818v1> (cited 10 July 2024).
- [13] Vu, D.T., 2011. The Role of Mangroves for Reducing High Waves During Typhoon in Dai Hop (Kien Thuy, Hai Phong). *Vietnam Journal of Marine Science and Technology*. 11(1), 43–55. (In Vietnamese)
- [14] Mazda, Y., Magi, M., Ikeda, Y., et al., 2006. Wave reduction in a mangrove forest dominated by *Sonneratia* sp. *Wetlands Ecology and Management*. 14, 365–378.
- [15] Suzuki, T., Zijlema, M., Burger, B., Meijer, M.C., Narayan, S., 2012. Wave dissipation by vegetation with layer schematization in SWAN. *Coastal Engineering*. 59(1), 64–71.
- [16] Horstman, E.M., Dohmen-Janssen, C.M., Narra, P.M.F., et al., 2014. Wave attenuation in mangroves: a quantitative approach to field observations. *Coastal engineering*, 94, 47–62.
- [17] Butera, M.K., 1983. Remote Sensing of Wetlands. *IEEE Transactions on Geoscience and Remote Sensing*. GE-21(3), 383–392.
- [18] Ghosh, M., Kumar, L., Roy, C., 2016. Mapping Long-Term Changes in Mangrove Species Composition and Distribution in the Sundarbans. *Forests*. 7(12), 305. DOI: <https://doi.org/10.3390/f7120305>
- [19] Karakis, S., Marangoz, A., Buyuksalih, G., 2006. Analysis of segmentation parameters in cognition software using high resolution quickbird ms imagery. *Proceedings of The ISPRS Workshop on Topographic Mapping from Space; February 14-16, 2006; Ankara, Turkey*. pp. 14–16.
- [20] O'Reilly, J.E., Maritorena, S., Siegel, D., O'Brien, M.C., Toole, D., Mitchell, B.G., 2000. Ocean color chlorophyll a algorithms for SeaWiFS, OC2, and OC4: Version 4. *SeaWiFS Postlaunch Calibration and Validation Analyses*. 11, 9–23.
- [21] Subramaniam, A., Brown, C.W., Hood, R.R., et al., 2001. Detecting *Trichodesmium* blooms in SeaWiFS imagery. *Deep Sea Research Part II: Topical Studies in Oceanography*. 49(1–3), 107–121.
- [22] Melin, F., 2009. Global Distribution of the Random Uncertainty Associated With Satellite-Derived Chl a. *IEEE Geoscience and Remote Sensing Letters*. 7(1), 220–224.
- [23] Gitelson, A.A., Dall'Olmo, G., Moses, W., et al., 2008. A Simple semi-analytical model for remote estimation of chlorophyll-a in turbid waters: Validation. *Remote Sensing of Environment*. 112(9), 3582–3593.
- [24] Al-Naimi, N., Raitzos, D.E., Ben-Hamadou, R., et al.,

2017. Evaluation of Satellite Retrievals of Chlorophyll-a in the Arabian Gulf. *Remote Sensing*. 9(3), 301.
- [25] Sivakumar, R., Prasanth, B.S.V., Ramaraj, M., 2022. An empirical approach for deriving specific inland water quality parameters from high spatio-spectral resolution image. *Wetlands Ecology and Management*. 30(2), 405–422.
- [26] Jalbuena, R.L., Peralta, R.V., Tamondong, A.M., 2015. Object-based image analysis for mangroves extraction using LIDAR datasets and orthophoto. *Proceedings of The Asian Association on Remote Sensing (AARS) Proceedings, 24-28 October 2015, Quezon City, Metro Manila Philippines*, pp.1-8
- [27] Cárdenas, N.Y., Joyce, K.E., Maier, S.W., 2017. Monitoring mangrove forests: Are we taking full advantage of technology?. *International Journal of Applied Earth Observation and Geoinformation*. 63(310), 1–14.
- [28] Thanh C, N., An T, D., Khuong NT, T., 2022. Monsoonal sediment transport along the subaqueous Mekong Delta: An analysis of surface sediment grain-size changes. *Ocean Systems Engineering*. 12(4), 403–411.
- [29] Kavzoglu, T., Yildiz, M., 2014. Parameter-Based Performance Analysis of Object-Based Image Analysis Using Aerial and Quikbird-2 Images. *ISPRS Annals of Photogrammetry, Remote Sensing and Spatial Information Sciences*. 2(7), 31–37.
- [30] Lee, S.K., Dang, T.A., Tran, T.H., 2018. Combining rainfall–runoff and hydrodynamic models for simulating flow under the impact of climate change to the lower Sai Gon-Dong Nai River basin. *Paddy and Water Environment*. 16, 457–465.
- [31] Baatz, M., Schape, A., 2000. Multiresolution segmentation: an optimization approach for high quality multiscale image segmentation. In: Strobl, J., Blaschke, T., Griesbner, G. (Eds.). *Angewandte geographische informationsverarbeitung, XII*. Wichmann Verlag: Karlsruhe, Germany. p. 2-1.